Available online at www.sciencedirect.com

SciVerse ScienceDirect

Ceramics International 38 (2012) 1255–1260

CERAMICS
INTERNATIONAL

www.elsevier.com/locate/ceramint

Growth characteristics of hierarchical ZnO structures prepared by one-step aqueous chemical growth

C.Y. Kuan [a], M.H. Hon [a,b], J.M. Chou [c], I.C. Leu [d,*]

[a] *Department of Materials Science and Engineering, National Cheng Kung University, Tainan 701, Taiwan, ROC*
[b] *Research Center for Energy Technology and Strategy, National Cheng Kung University, Tainan 701, Taiwan, ROC*
[c] *Department of Materials Science and Engineering, I-Shou University, Kaohsiung Hsien 840, Taiwan, ROC*
[d] *Department of Materials Science, National University of Tainan, 33, Sec. 2, Shu-Lin St., Tainan 700, Taiwan, ROC*

Received 21 July 2011; received in revised form 26 August 2011; accepted 27 August 2011

Abstract

By varying the initial precursor concentrations of (KOH/Zn$(NO_3)_2$ $6H_2O$) without addition of surfactants, the branched nanostructures with different growth characteristics can be obtained. In this study, the growth behavior of the three-dimensional hierarchical structure arrays varied from randomly oriented to well-defined sixfold symmetry by altering pH value of the solution and the related effect of erosion phenomenon have been illustrated. In summary, the hierarchical structures with different morphologies can be obtained on preformed Zn microtips through a simple one-step solution method.

Keywords: D. ZnO; Hierarchical; Solution

---

1. Introduction

In the past, the formation of semiconductor nanostructures with controlled dimension and different morphologies is the point of research. Nanoscale structures are expected to be manipulated into well-defined configuration in order to build integrated systems. Different nanostructures synthesized from semiconductor materials are of particular interest primarily because of their unique physical properties. Among the promising optoelectronic semiconductors, ZnO with a direct wide band gap (3.37 eV) and high exciton binding energy (60 meV), is one of the most important functional materials. So far, the growth of controlled microstructures, especially the novel well-organized hierarchical structures, has been performed by several methods, such as, conventional thermal evaporation and condensation method [1], solution-phase growth [2], and electrochemical deposition [3]. Gas-phase synthesis techniques have been used to grow branched nanocrystals for several material systems [4–6], but the equipments are complex, expensive, and consume high levels of energy. Many types of branched nanocrystals have also been produced with solution-phase synthesis process, which offers the potential for low-cost, industry-scale manufacturing [2,7,8]. However, the branched crystals by solution-phase synthesis are often in the form of precipitated powder and deposited randomly. Several studies regarding the direct oxidation of metallic zinc foil by solvothermal or solution approaches have been reported [9,10]. The various chemical methods have been used to obtain one-dimensional structures, and the formation mechanisms have also been suggested. Besides, the soft template, such as, cetyltrimethylammonium bromide (CTAB), polyethylene glycols (PEG), and poly(styrene sulfonic acid) (PSS), are also adopted for preparing three-dimensional hierarchical structures on Zn foil [11]. The 3D hierarchical structures obtained by soft template do not align uniformly on the metallic substrates. It is suggested that the growth of orientated, anisotropic, and well-defined 3D hierarchical structures on Zn foil is not easy to control.

In this research, the single-crystalline Zn pyramid microstructures prepared by anodic etching on polycrystalline Zn foil are served as a template for nanostructure growth [12]. A new hierarchical morphology has been successfully obtained by

---

* Corresponding author.
E-mail address: icleu@mail.mse.ncku.edu.tw (I.C. Leu).

0272-8842/$36.00 © 2011 Elsevier Ltd and Techna Group S.r.l. All rights reserved.
doi:10.1016/j.ceramint.2011.08.057

Table 1
Concentration of precursor and pH value for aqueous chemical growth.

	Sample			
	A	B	C	D
KOH(M)	0.8	2.0	4.0	6.0
$Zn(NO_3)_2 \cdot 6H_2O$(M)	0.1	0.25	0.5	0.75
pH value	10.9	11.3	13.3	13.8

one-step aqueous chemical growth method. By increasing the surface area, the novel hierarchical Zn/ZnO structures may find applications such as gas sensing, field emission, photocatalysis, and antireflection properties. The different morphologies of branched growth obtained by controlling the initial composition of solution are also discussed. The formation mechanisms for the hierarchical structures including shelled oxide layer formation and branched nanostructure growth are also elucidated. For solution-phase approach, the surface of metallic foil is eroded during synthesis and the interface between substrates and nanostructures are rough [13]. In the study, both the well-defined sixfold and radially oriented hierarchical structures are obtained under different reaction time and temperature. In this report, we present an analysis for the effects of the pH value of growth solution and the erosion phenomena on the morphologies of hierarchical structures. This work may provide a new rationale pertaining to the design and preparation of ordered nanostructures by a simple solution method, and it has the potential for scale-up preparation.

2. Experimental procedure

The single-crystalline metallic Zn pyramid microstructures, i.e., microtips, were prepared by anodic etching on polycrystalline Zn foil [12], which was conducted in a solution of NH_4Cl/H_2O_2 with molar ratio of 32 using a constant current density of 55 mA cm^{-2} for 60 s. Aqueous chemical growth solution with different compositions was composed of KOH and $Zn(NO_3)_2 \cdot 6H_2O$ as shown in Table 1 at a fixed volume ratio of 1:1. The synthesis process was performed under different times (5, 10, 15, 20, 30 min) and temperatures (RT, 40, 50, 60 °C). Then, the samples for cross-sectional TEM were prepared by focused ion beam (FIB, SMI 3050). The hierarchical structures thus obtained were characterized by field emission scanning electron microscopy (FE-SEM, JSM-7000F, Jeol), and the structural characteristics were studied by transmission electron microscopy (FEG-TEM, Tecnai F20 G2 MAT, FEI).

3. Results and discussion

Fig. 1 shows the SEM observation for different ZnO morphologies obtained using different precursor concentrations as shown in Table 1, and the samples are designated as samples A, B, C, and D. Under whatever the initial solution conditions, the self-assembled three-dimensional hierarchical structures on Zn foil are obtained. The most interesting phenomenon in secondary branch growth is the transition from randomly oriented nuclei to preferentially oriented branches with increasing precursor concentration ($KOH/Zn(NO_3)_2$) above 4.0/0.5 (for samples C

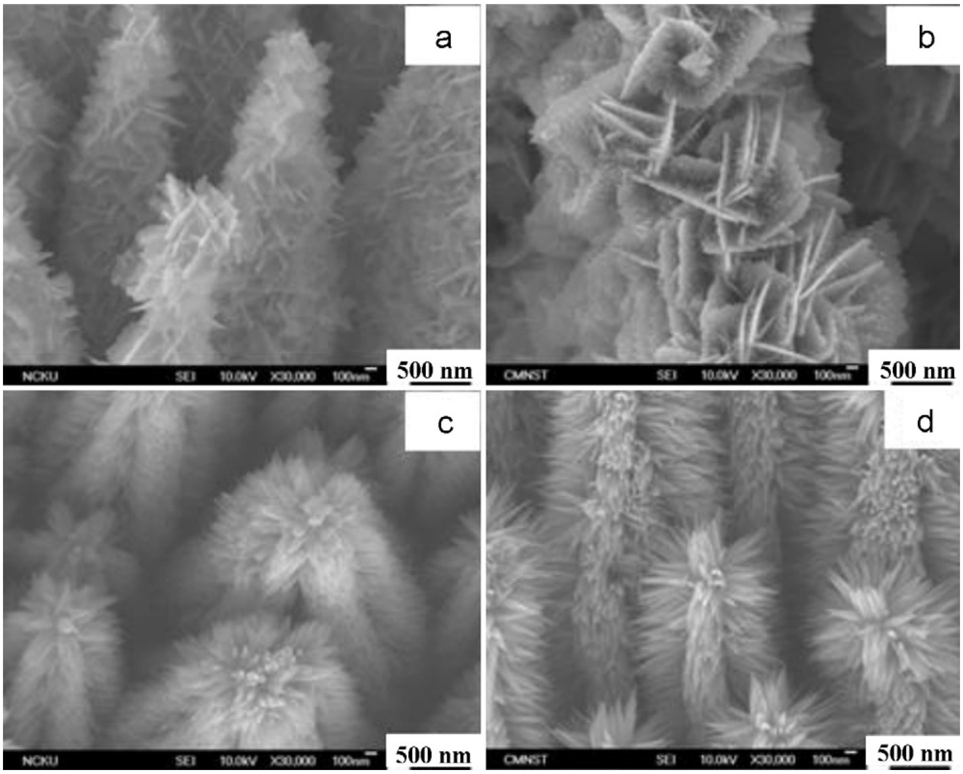

Fig. 1. SEM images of hierarchical structures prepared by different precursor concentration ($KOH/Zn(NO_3)_2$) of (a) 0.8/0.1, (b) 2.0/0.25, (c) 4.0/0.5, and (d) 6.0/0.75 at room temperature for 10 min.

and D). Besides, a modification of the morphology from sheet-like, to flower-like structures, and finally to nanowires at various precursor concentrations for the branched ZnO nanostructures is obtained. In solution system, by adjusting the experimental parameters, such as, additional soft templates, the molar ratio of chemical agents, pH of solution, and the nature of the substrate, many ZnO structures with different morphologies and size can be obtained [14,15]. In general, the nanostructures with different morphologies have usually been prepared by the addition of the structure-modifying agents [16,17], and the agents may form a chelating ligand with ions of Zn^{2+} or O^{2-}, which will preferentially bind to the energetically polar surface. Such absorption can reduce the surface energy of the crystalline planes; therefore, the axial growth of ZnO nanocrystals is drastically suppressed. In the present study, no additional surfactant or capping agent is used during the growth process, and both the molar ratio of chemical agents ($OH^-/Zn^{2+} = 8$) and the nature of substrates are fixed. The main influences of different chemical solution conditions on various morphologies can be attributed to the changed pH values of solution which is determined by the concentration of Zn^{2+} and OH^-. In other words, the supersaturated solution is a prerequisite for crystallization and the level of supersaturation is important in determining the final crystal morphology. The initial pH value for these four reaction mixtures is shown in Table 1, with the values of 10.9, 11.3, 13.3, and 13.8, respectively. In comparison with the SEM observation, the sheet-like ZnO is obtained under the lower pH value (10.9) condition, then with increasing the pH value to 13.3, the morphology changes to nanowires. The pH value represents the concentration of OH^- ions in ACG process, and the various pH values of reaction solution probably results in different nucleation and growth rates [18]. The effect of pH value on morphology development has also been reported [19]. Under different solution conditions, one-dimensional ZnO nanorods are developed into two-dimensional nanostructures with increasing pH value. However, in the present study, an opposite trend to others reported in the literature is observed for the variation of morphology with increasing pH value. It is well-known that, to grow ZnO crystals by the chemical solution approaches, the basic growth unit is $[Zn(OH)_4]^{2-}$. The growth mechanism of ZnO by ACG method on Zn foil has been reported, and the importance of $[Zn(OH)_4]^{2-}$ ions on growing ZnO crystal has been indicated [9]. The mechanisms can be simply represented by the following reactions [10]: $Zn + 2H_2O + 2OH^- \rightarrow Zn(OH)_4^{2-} + H_2$, $Zn(OH)_4^{2-} \rightarrow ZnO + H_2O + 2OH^-$. In a solution at a higher pH value condition, the concentration of growth unit of $[Zn(OH)_4]^{2-}$ has been increased, as predicted by the above equation. The influence of the negatively charged $[Zn(OH)_4]^{2-}$ on the nanostructured ZnO growth characteristics has been reported [20]. The basic growth unit may be preferentially attracted to the growth facet and results in the longitudinal growth along the $\langle 0\,0\,0\,1 \rangle$ direction [20]. In the present report, comparison of ZnO nanostructure morphologies as a function of the initial precursor conditions reveals the effect of pH value on the ZnO growth characteristics. Below a certain pH limit, i.e., at pH value of 11.3, the reaction occurs vigorously, and as a result the growth occurs in both lateral and longitudinal directions in an uncontrolled manner, resulting in the formation of flower-like ZnO morphology as shown in Fig. 1(b). The result indicates that there is an appropriate range of the pH value for the growth of well-aligned sixfold ZnO branches, i.e., above 13.3 on single-crystalline Zn microtip arrays under the growth conditions. In summary, by altering the pH value, the growth characteristics of branches change from two-dimensional to one-dimensional nanostructures.

To investigate the growth process of the ZnO hierarchical structures, the experiments for different reaction time and temperature are conducted using precursor concentration ($KOH/Zn(NO_3)_2$) of 4.0/0.5. An enlarged section for samples prepared at the early stages indicates that the surfaces are fully covered by short nanowires, and the dense and tapered ZnO nanowires grow on the facets of the pyramid Zn microtips as shown in Fig. 2(a). After reaction for 5 min, uniform ZnO nanowires with an average length of 210 nm are grown from the facets, and a self-assembled sixfold symmetry morphology is obtained. In addition, in Fig. 2(b), an erosion phenomenon is observed at the tips of microtips under the process of forming hierarchical structure. With reaction time for 20 min, the clear erosion phenomenon by agitating under ACG reaction is observed in Fig. 2(c), and the direction of collapsed hierarchical structures is in agreement with the condition of solution agitation. With further increasing reaction time to 25 min(not shown here), not only the collapsed hierarchical structures are obtained, but also radially oriented hierarchical structures are observed. In this study, the metal foil acts both as the reactant and the supporting substrate in solution, the growth units transport to a certain region near the substrate and then precipitate nanostructures on the surface [13]. The slight erosion phenomena on the metallic foil are observed under agitated solution, and the surface of the metal substrate is not smooth [13]. These results demonstrate that the erosion mechanism accompanies with ACG reaction under agitation. In order to clarify the erosion phenomenon, a blank experiment without stirring is practiced. The SEM observation of the blank experiment exhibits a radially oriented Zn/ZnO hierarchical structure. From the observation, the length of the radial arrays can be maintained under ACG processes without solution agitation. The results suggest that the erosion phenomenon at the corner of the microtips comes from the solution, and results in the growth of radial arrays; however, the collapsed phenomenon results from the solution with agitation. With increasing reaction temperature above 50 °C as shown in Fig. 2(d), the well-defined sixfold hierarchical structures cannot be maintained, but only the radially oriented hierarchical structure arrays are observed. The results illustrate that the erosion phenomenon is more obvious with increasing reaction temperature. Besides, from the cross-sectional TEM observation, as shown in Fig. 2(e), a resembling circle around the center can be obtained. The results indicate that the erosion prefers to take place at the corner of the Zn microtips and to blunt the contour of the edge, and finally results in the growth of radially oriented hierarchical structure arrays. In other words, the preferred nucleation sites for branch growth are the facets of the Zn microtip arrays, i.e., the sixfold hierarchical structures are

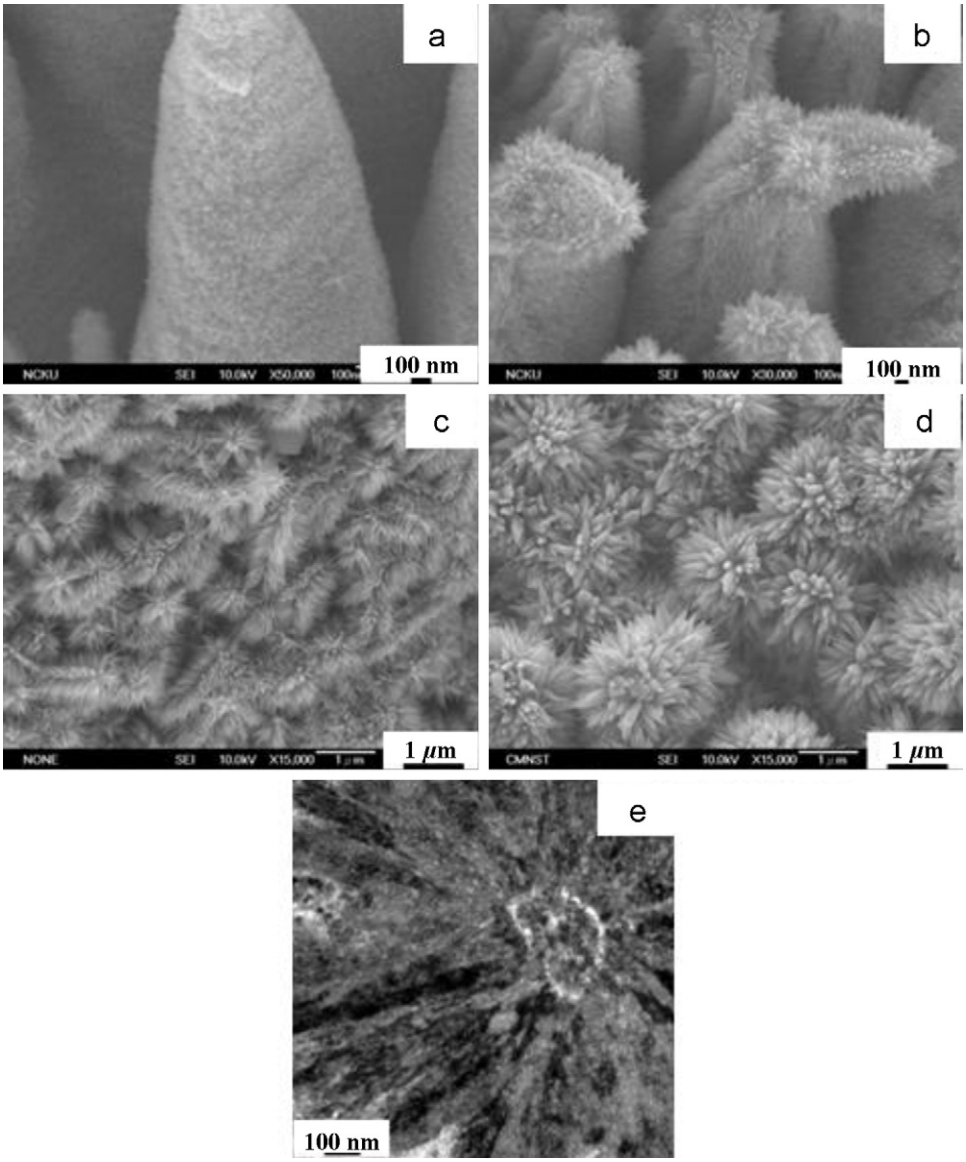

Fig. 2. The microscopy for hierarchical structure on Zn microtips at precursor concentration of KOH/Zn$(NO_3)_2$ = 4.0/0.5 for different reaction time and temperature under solution agitation, (a) 1, (b) 5, (c) 20 min, (d) 50 °C, and (e) is the cross-sectional TEM is obtained from (d).

obtained. Then, as the corners of the Zn microtips are eroded by the chemical solution and the new nucleation events occur at the eroded round corners.

To realize the growth characteristics of the branched nanostructures for sheet- and flower-like products, the HRTEM analyses are performed as shown in Fig. 3. The low magnification images and the diffraction patterns are arranged as insets in the high resolution images. In Fig. 3(a), the sheet-like nanostructures are removed from the sample A(as designated in Table 1) with length and width about 250 nm and 300 nm, respectively. Electron diffraction analysis indicates that the zone axis is along $[2\bar{1}\bar{1}0]$, and the growth directions of sheet-like nanostructures are along $[0001]$, $[10\bar{1}0]$, and $[01\bar{1}1]$. Fig. 3(b) shows the HRTEM observation of sample C obtained by focused ion beam micromachining. From the cross-sectional TEM observation, it clearly demonstrates that the branched nanostructures are composed of nanosheet and nanowires. The thickness of nanosheet and diameter of nanowire are about 50 nm and 30–40 nm, respectively. Besides, the diffraction pattern results indicate that the nanosheet and nanowire of flower-like branches are with well-defined epitaxial relationship. The epitaxial relationship between sheets and nanowires can be determined by the SAED analyses. The nanowires grow from nanosheets surface exhibiting an angle of about 115° to the nanosheet growth direction. In conclusion, the morphology evolution of branched structure is consistent with the effect of pH, and the epitaxial relationship for flower-like structures has also been illustrated.

The cross-sectional TEM observation of the sample with sixfold hierarchical structures is obtained for sample prepared at precursor concentration (KOH/Zn$(NO_3)_2$) of 4.0/0.5, as shown in Fig. 4. The TEM images of the central region for the well-defined hierarchical structures exhibit the sixfold symmetry as shown in Fig. 4(a), and the result is in agreement with SEM observation.

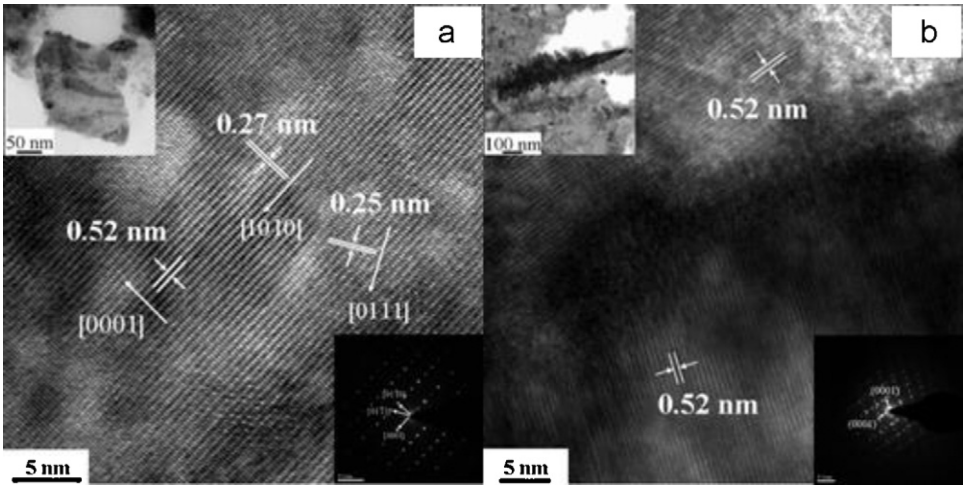

Fig. 3. HRTEM analyses of growth characteristics for sheet- and flower-like branches under different pH value. (a) Sample A ($KOH/Zn(NO_3)_2 = 0.8/0.1$, and (b) sample B ($KOH/Zn(NO_3)_2 = 2.0/0.25$). Insets are bright-view images and selected area electron diffraction patterns.

Obviously, a shell structure in Fig. 4(a), is formed at the interface between Zn microtips and ZnO nanowires, and the length of branches is uniform. In addition, the branched ZnO nanowires are aligned on the facet of Zn stem and also exhibit sixfold symmetry. The result also demonstrates that the growth of hierarchical arrays into sixfold symmetry is because of the hexagonal symmetry of the major core, i.e., the microtips. The high-resolution image and selected-area electron diffraction (SAED) pattern (as shown in Fig. 4(b)) indicate that the lattice spacing of 0.52 nm corresponds to the *d* spacing of the (0 0 0 1)

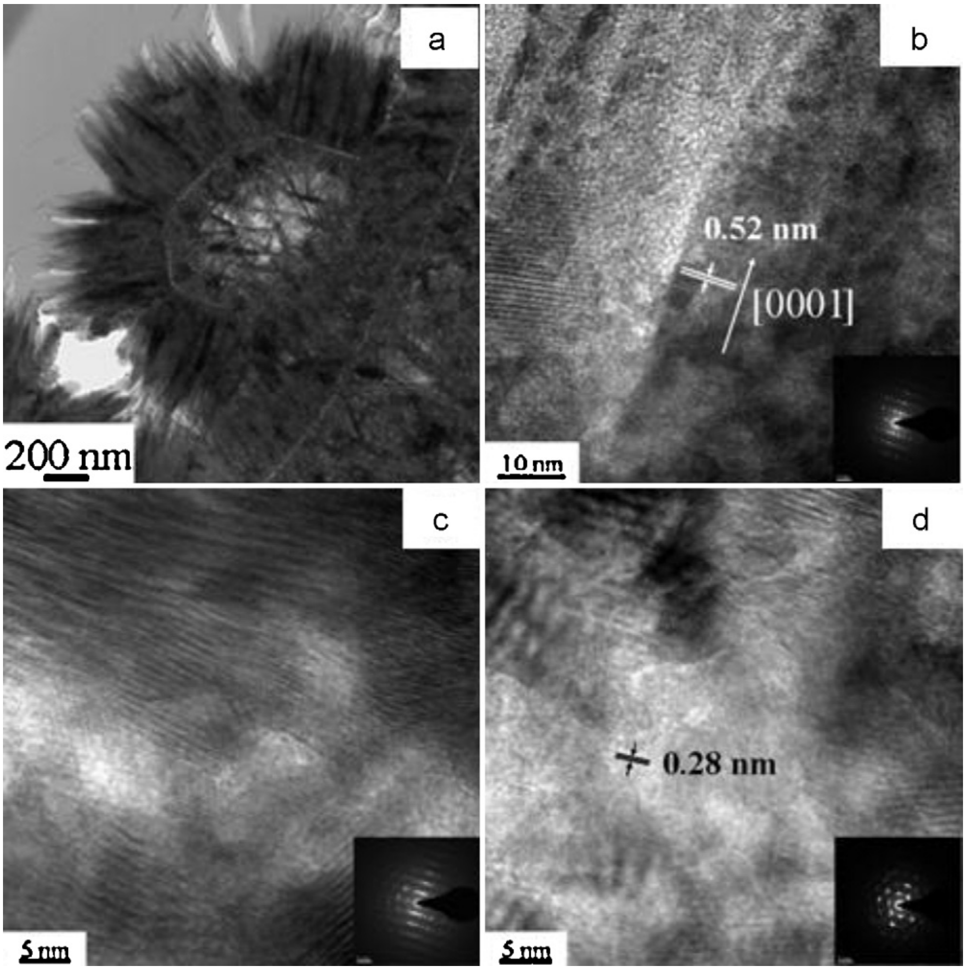

Fig. 4. TEM analyses of orientation relationship on core–shell (Zn microtips/ZnO nanowires) structures. (a) Bright-field view, and HRTEM on (b) branched ZnO nanowires, (c) interface between shelled and branched ZnO, and (d) shelled dense ZnO film.

crystal planes, and the growth direction is along [0 0 0 1]. From the HRTEM observation of Fig. 4(c), the interface exhibits some defects, such as, stacking faults, dislocation and Moiré fringe pattern [21,22], owing to the mismatch between planes of shell and branches. As shown in Fig. 4(d) is the atomically resolved TEM image taken from the shell area, which clearly displays its single-crystalline nature. A 0.28 nm separation between the two neighboring lattice fringes corresponds to the ZnO $\{10\bar{1}0\}$ lattice spacing, and the [0 0 0 1] zone axis is depicted. The epitaxial relationship between ZnO branches and oxide layer, which can be determined from the SAED in Fig. 4, is $[2\bar{1}\bar{1}0]_{\text{branches}}//[0001]_{\text{shell}}$. The epitaxial relationship is also confirmed in the local HRTEM image and diffraction pattern of the interface between ZnO branches and layer shown in Fig. 4(c). As discussed above, the surface of the Zn microtips gradually grows into shelled ZnO layer, then the branched nanostructures nucleate and grow from the oxide layer. The creation of new nucleation events that produce secondary crystal growth is a critical step for the success of the development of multi-level hierarchical structures. Moreover, the antireflection properties of the specific hierarchical structures have been preliminarily evaluated, and the reflectance can be decreased by 40% with the grown ZnO nanostructures on Zn microtips. The structure characteristics and properties of the ZnO hierarchical structures are expected to find wide applications as photoelectrodes in solar cell devices.

4. Conclusion

In summary, the present chemical approach offers a simple and scalable method for the growth of a symmetrical hierarchical array under a mild process environment. At room temperature and ambient pressure, highly regular ZnO nanosheets or nanowires can be prepared. Different morphologies can be obtained by simply varying precursor concentrations within a certain pH range. The morphology develops from nanosheets to nanowires by changing the solution pH value to 13.3. It is suggested that the nanostructure morphologies can be determined by tuning the precursor concentration. Besides, the growth characteristics have also been illustrated by TEM analyses, and the orientation relationship of the flower-like nanostructures has been demonstrated. With increasing either the reaction time or temperature, the 3D sixfold hierarchical structure cannot be obtained owing to the erosion phenomenon. The SEM and TEM observations illustrate that the erosion phenomenon takes place first from the corner of Zn microtips and an otherwise radially oriented hierarchical structure is obtained. Besides, the epitaxial relationship for well-defined core-shelled hierarchical arrays between branches and shelled layer is confirmed as $[2\bar{1}\bar{1}0]_{\text{branches}}//[0001]_{\text{shell}}$.

Acknowledgement

The financial support of this study from the National Science council (NSC 99-2221-E-024-004 and NSC 97-2221-E-239-028) and MoE ATU plan is greatly appreciated.

References

[1] P.X. Gao, Z.L. Wang, Nanopropeller arrays of zinc oxides, Appl. Phys. Lett. 84 (2004) 2883–2885.

[2] T.L. Sounart, J. Liu, J.A. Voigt, M. Huo, E.D. Spoerke, B. Mckenzie, Secondary nucleation and growth of ZnO, J. Am. Chem. Soc. 129 (2007) 15786–15793.

[3] L.F. Xu, Q.W. Chen, D.S. Xu, Hierarchical ZnO nanostructures obtained by electrodeposition, J. Phys. Chem. C 111 (2007) 11560–11565.

[4] Y. Baek, Y. Song, K. Yong, A novel heteronanostructure system: hierarchical W nanothorn arrays on WO_3 nanowhiskers, Adv. Mater. 18 (2006) 3105–3110.

[5] C. Ye, L. Zhang, X. Fang, Y. Wang, P. Yan, J. Zhao, Hierarchical structure: silicon nanowires standing on silica microwires, Adv. Mater. 16 (2004) 1019–10233.

[6] X.J. Mao, S.W. Wang, S.Z. Shimai, Porous ceramics with Tri-modal pores prepared by foaming and starch consolidation, Ceram. Int. 34 (2008) 107–112.

[7] S. Komarneni, M. Bruno, E. Mariani, Synthesis of ZnO with and without microwaves, Mater. Res. Bull. 35 (2000) 1843–1847.

[8] T. Zhang, W. Dong, M.K. Brewer, S. Konar, R.N. Njabon, Z.R. Tian, Site-specific nucleation and growth kinetics in hierarchical nanosyntheses of branched ZnO crystallites, J. Am. Chem. Soc. 128 (2006) 10960–10968.

[9] S. Kar, A. Dev, S. Chakrabarti, S. Chaudhuri, Simple solvothermal route to synthesized ZnO nanosheets, nanonails, and well-aligned nanorod arrays, J. Phys. Chem. B 110 (2006) 17848–17853.

[10] X.F. Wu, H. Bai, C. Li, G. Lu, G.Q. Shi, Controlled one-step fabrication of highly oriented ZnO nanoneedle/nanorods arrays at near room temperature, Chem. Commun. (2006) 1655–1657.

[11] J.P. Liu, X.T. Huang, Y.Y. Li, K.M. Sulieman, F.L. Sun, X. He, Selective growth and properties of zinc oxide nanostructures, Scr. Mater. 55 (2006) 795–798.

[12] C.Y. Kuan, J.M. Chou, I.C. Leu, M.H. Hon, Formation and field emission property of single-crystalline Zn microtip arrays by anodization, Electrochem. Commun. 9 (2007) 2093–2097.

[13] Z.Q. Li, Y. Ding, Y.J. Xiong, Q. Yang, Y. Xie, Room-temperature surface-erosion route to ZnO nanorod arrays and urchin-like assemblies, Chem. Eur. J. 10 (2004) 5823–5828.

[14] D. Vernardou, G. Kenanakis, S. Couris, E. Koudoumas, E. Kymakis, N. Katsarakis, pH effect on the morphology of ZnO nanostructures grown with aqueous chemical growth, Thin Solid Films 515 (2007) 8764–8767.

[15] S. Yamabi, H. Imai, Growth conditions for wurtzite zinc oxide films in aqueous solution, J. Mater. Chem. 12 (2002) 3773–3778.

[16] N.X. Wang, C.H. Sun, Y. Zhao, S.Y. Zhou, P. Chen, L. Jiang, Fabrication of three-dimensional ZnO/TiO_2 heteroarchitectures via a solution process, J. Mater. Chem. 18 (2008) 3909–3911.

[17] A.I. Inamdar, S.H. Mujawar, V. Ganesan, P.S. Patil, Surfactant-mediated growth of nanostructured zinc oxide thin films via electrodeposition and their photoelectrochemical performance, Nanotechnology 19 (325706) (2008) 7.

[18] U. Pal, P. Santiago, Controlling the morphology of ZnO nanostructures in a low-temperature hydrothermal process, J. Phys. Chem. B 109 (2005) 15317–15321.

[19] H.K. Sun, M. Luo, W.J. Weng, K. Cheng, P.Y. Du, G. Shen, G.R. Han, Room-temperature preparation of ZnO nanosheets grown on Si substrates by a seed-layer assisted solution route, Nanotechnology 19 (125603) (2008) 5.

[20] Y.J. Lee, T.L. Sounart, J. Liu, E.D. Spoerke, Tunable arrays of ZnO nanorods to nanoneedles via seed layer and solution chemistry, Cryst. Growth Des. 8 (2008) 2036–2040.

[21] Y. Ding, X.Y. Kong, Z.L. Wang, Interface and defect structure of Zn–ZnO core–shell heteronanobelts, J. Appl. Phys. 95 (2004) 306–310.

[22] Y.H. Wong, Q. Li, Study of the crystallinity of ZnO in the Zn/ZnO nanocable heterostructures, J. Mater. Chem. 14 (2004) 1413–1418.